CONF-931121--1

LA-UR-93-1058
N-6-93-R109

Los Alamos National Laboratory is operated by the University of California for the United States Department of Energy under contract W-7405-ENG-36

TITLE: NUMERICAL MODELING OF THE EFFECT OF SURFACE TOPOLOGY ON THE SATURATED POOL NUCLEATE BOILING CURVE

AUTHOR(S): Cetin Unal
Kemal O. Pasamehmetoglu

SUBMITTED TO: 1993 ASME Winter Annual Meeting
November 28–December 3, 1993
New Orleans, Louisiana

DISCLAIMER

Los Alamos
Los Alamos National Laboratory
Los Alamos, New Mexico 87545

NUMERICAL MODELING OF THE SURFACE TOPOGRAPHY EFFECTS ON THE SATURATED POOL NUCLEATE BOILING CURVE

by

Cetin Unal and Kemal Pasamehmetoglu

Nuclear Technology and Engineering Division
Engineering and Safety Analysis Group
Los Alamos National Laboratory
Los Alamos, NM 87545

ABSTRACT

A numerical study of saturated pool nucleate boiling with an emphasis on the effect of surface topography is presented. The numerical model consisted of solving the three-dimensional transient heat conduction equation within the heater subjected to nucleate boiling over its upper surface. The surface topography model considered the distribution of the cavity and cavity angles based on exponential and normal probability functions. Parametric results showed that the saturated nucleate boiling curve shifted left and became steeper with an increase in the mean cavity radius. The boiling curve was found to be sensitive to the selection of how many cavities were selected for each octagonal cell. A small variation in the statistical parameters, especially cavity radii for smooth surfaces, resulted in noticeable differences in wall superheat for a given heat flux. This result indicated that while the heat transfer coefficient increased with cavity radii, the cavity radii or height alone was not sufficient to characterize the boiling curve. It also suggested that statistical experimental data should consider large samples to characterize the surface topology. The boiling curve shifted to the right when the cavity angle was obtained using a normal distribution. This effect became less important when the number of cavities for each cell was increasing because the probability of the potential cavity with a larger radius in each cell was increased. When the contact angle of the fluid decreased

for a given mean cavity radii, the boiling curve shifted to the right. This shift was more pronounced at smaller mean cavity radii and decreased with increasing mean cavity radii.

NOMENCLATURE

a_1	Empirical constant
C_1	Empirical constant
N_m	Mean number of cavities per cell
N_T	Total number of cavities
q	Surface-time averaged wall heat flux (W/m^2)
R_c	Cavity mouth radius (mm)
$R_{c,m}$	Mean cavity mouth radius (mm)
R_{max}	Maximum cavity radius (mm)
R_z	Cavity height (mm)
pfd	Probability density function
β	Half-cone angle
β_m	Mean half-cone angle
ΔT_w	Surface-time averaged wall superheat (°C)
θ	Contact angle
σ_N	Standard deviation for number of cavities per cell
σ_β	Standard deviation for cavity cone angle

I. INTRODUCTION

A complete understanding of the nucleate boiling process continues to elude engineers and scientists despite more than half a century of research. This situation possibly arises because there are an abundant number of parameters (quite often dependent with unknown functional interrelations) affecting the phenomenon. It is almost impossible to design experiments where these parameters may be varied and controlled independently from each other. Fortunately, in recent years, there is

an increased trend where the experiments are complemented with detailed modeling so that parametric dependencies and data reduction may be better accomplished.

As part of that effort, we developed a computer model where the saturated pool nucleate boiling over a horizontal surface is simulated (Pasamehmetoglu and Nelson 1991a). Along with sample nucleate boiling calculations, the model is described in a recent publication (Pasamehmetoglu 1992). However, this paper was aimed primarily at illustrating the various aspects of the model without targeting any specific questions pertinent to pool nucleate boiling phenomenon. In this respect, the present paper is a continuation of the previous ones (Pasamehmetoglu and Nelson 1991b, Pasamehmetoglu 1992) and it is aimed primarily at investigating the surface topography effects on the nucleate boiling curve.

The surface conditions strongly affect the nucleate boiling curve. Starting with the work of Jacob and co-workers in the early 1930s (cited by Jacob 1949), there is an abundance of mostly experimental studies in the literature where the effects of surface conditions on the nucleate boiling curve are investigated. A comprehensive literature review on the subject would be extensively lengthy to be included in this paper, and it is outside the scope of our discussion. As examples of such studies, the readers are referred to the study of Bartheau (1992), Chowdhury and Winterton (1985), and Dhir (1990).

Typically surface conditions that influence the nucleate boiling are listed in the literature as the surface roughness and contact angle (Chowdhury and Winterton 1985). The contact angle may influence the nucleate boiling through a number of mechanisms. The number of potential sites is a function of contact angle. As shown by Bankoff (1958), the conical cavities will be potential sites if $\theta > 2\beta$, where θ is the contact angle and β is the half-cone angle. Thus, larger contact angles result in more potential sites and thus, in more active sites, as observed

experimentally by Wang and Dhir (1991). Contact angle influences the formation and evaporation of the microlayer. The mechanisms for this phenomenon are not fully understood. Finally, increasing the contact angle may increase the bubble departure diameter, thus influencing the bubble emission frequency from a given site. Changing the contact angle over a narrow range appears to have no serious consequences on the nucleate boiling curve (Chowdhury and Winterton 1985). However, Wang and Dhir (1991) reported a noticeable shift of the boiling curve to the left (enhanced heat transfer) when the contact angle is changed from 18° to 90° for boiling of saturated water over a copper surface. Contact angle is a function of the surface energies of the fluid and the heater material and is strongly influenced by the surface oxidation. Also, one has to carefully distinguish between static and dynamic contact angles that influence different mechanisms of the nucleate boiling phenomenon. In the current paper, we do not explicitly address the nature of the contact angle problem. Throughout our discussion, it is assumed that the contact angle is explicitly known and considered as a apparent static contact angle. We incorporate this known value into our analysis to determine the potential active cavities using Bankoff's (1958) flooding criterion.

Surface roughness influences the nucleate boiling curve by affecting the number of cavities and the size, shape, and spatial distribution of the cavities. However, Chowdhury and Winterton (1985) indicated that surface roughness quantified by center line average (CLA) may be a meaningless parameter. By comparing the anodized and unanodized surfaces with the same measure of roughness, they argued that the number of cavities and not the roughness was the important parameter. In general, the surface roughness as a single parameter is a statistical representation of the surface topography (Thomas 1981). However, hidden within this number are a number of parameters that have a direct influence on the boiling curve. Without the capability of differentiating among those

parameters and their effects on the boiling curve, the roughness as a single parameter has little universal meaning in terms of quantifying the boiling curve. To complicate matters even further, there appear to be different standards and/or measurement methods in quantifying the surface roughness (Thomas 1981), and one has to be careful in specifying the method associated with a given numerical value.

The parameters that characterize the surface roughness and that influence the nucleate boiling curve are as follows:

1. **The number of cavities on the surface.** This is a parameter that is not typically contained within the roughness measurement [CLA or root mean square (RMS)]. Furthermore, within the context of the nucleate boiling, how we count the number of cavities is not always clear. The example shown in Fig. 1 illustrates this point. Both configurations in (a) and (b) show two adjacent cavities. However, if we apply the gas entrapment mechanism suggested by Bankoff (1958), both cavities are capable of individual bubbles [Fig. (1-a)], whereas only a single bubble may be generated from both cavities [Fig. (1-b)].
2. **Cavity shape and characteristic dimensions.** The roughness magnitudes do not directly contain the shape information. The roughness typically quantifies one of the characteristic dimensions (height). However, on a natural surface, various cavity shapes are possible. In the boiling literature, cavity shapes are commonly idealized as conical and reservoir types for natural surfaces and cylindrical for artificially drilled surfaces. The shape of natural cavities is expected to significantly deviate from these idealized geometries. Two dimensions (mouth radius and height) are sufficient to characterize the conical and cylindrical cavities. Reservoir-

type cavities may be characterized using three dimensions (mouth radius, cavity radius, and height). Obviously, as the shape becomes more complex, the dimensionality of the cavity increases, and the problem quickly progresses into the domain of fractal geometry. However, in view of Bankoff's gas entrapment mechanism, the secondary patterns on the shape of the cavity may have little influence on the nucleate boiling curve (depending upon contact angle). For instance, conical and truncated conical cavities are shown in Fig. 2. Depending upon the contact angle, these two cavities may behave identically or quite differently during the boiling process. For the large contact angle of case (a), both cavities entrap gas. On the other hand, for the small contact angle in case (b), the conical cavity is capable of entrapping gas, whereas the truncated cone is completely flooded. Thus, how the shape of the cavities influences the boiling depends on the contact angle.

In the present paper, we try to address some of the questions pertinent to surface effects through numerical simulation. The study is aimed primarily at a parametric analysis. In that respect, we believe valuable information may be gained from such studies in terms of understanding the boiling curve behavior and in terms of interpreting the experimental data. On the other hand, we acknowledge that our numerical model is currently not capable of modeling all the details of a real boiling surface. While the model itself has certain limitations, the major deficiency is in our capability of defining a real surface (as evidenced by our discussion in the previous paragraphs).

In the next section, we provide a brief summary of the numerical model for a boiling surface. The surface topography model, which is used as an input to the boiling heat transfer model, is discussed subsequently.

II. BOILING HEAT TRANSFER MODEL

We developed a computer program to investigate the pool boiling phenomenon over a horizontal heater. The program consists of solving the three-dimensional transient heat conduction equation within the heater subjected to nucleate boiling over its upper surface, using a finite-control volume approach. The details of the program and its closure models are provided in our previous publications (Pasamehmetoglu and Nelson 1991a, 1991b, Pasamehmetoglu 1992). A summary is provided in this section.

The numerical grid contains octagonal cells. The size of the octagonal cells is determined by the maximum bubble departure diameter. In the current calculations, the bubble departure diameter is assumed to be independent of the heat flux over the range investigated. The departure diameter also is assumed to be constant spatially over the boiling surface. For saturated water at atmospheric pressure, the bubble departure diameter is computed to be ~2.4 mm, using the correlation of Cole and Rohsenhow (1969). Potential cavities are placed in the center of each octagonal cell. The program contains inception, growth, and departure models for the bubbles stemming from those cells. During the bubble waiting time, a transient conduction model for the liquid layer is used. Microlayer evaporation and dry spot formation is modeled during bubble growth. Isothermal and isobaric models are combined to characterize the bubble growth. During the isothermal stage, the microlayer evaporation is assumed to be solely responsible for bubble growth. When the bubbles grow to a given departure size, they depart. The cells that do not contain potential cavities are cooled by natural convection.

The current calculations are performed using a 1-mm-thick copper heater, and saturated water at atmospheric pressure was considered as the coolant. As mentioned before, the nucleate boiling takes places on the upper surface of the

heater. At the bottom surface, a constant heat flux is used for the results presented in this paper.

The major limitation of the numerical model in terms of modeling a true boiling surface results from the use of the finite-control volume approach with a fixed grid. Only a single cavity located at the cell center is allowed to participate in bubble emission. Modeling of multiple sites emitting intermittently under the projected area of a given bubble currently is not considered. Note that the cross-sectional size of the octagonal cells coincides with the size of a departing bubble. Within this cell, a spatially averaged temperature is computed. The lack of spatial temperature resolution in a given cell along with a fixed grid model makes it impossible to properly account for multiple cavities in an octagonal cell. To circumvent this problem, one can use very small grid sizes and allow a growing bubble to extend over multiple cells. However, our preliminary attempts in using this approach resulted in very expensive computations for a reasonably sized heater surface (because of the enormous number of computational cells that results from this approach). As a result, we decided to neglect the shortcomings in terms of spatial resolution under a growing bubble and the inability of modeling multiple sites in a computational cell of lateral dimension on the order of a few millimeters.

The calculations were run until stationary conditions were obtained. Typically, 2–3 s of problem time was enough to reach the stationary thermal conditions. The calculated values, such as wall superheat and heat flux, bubble density, and active nucleation site density were time averaged for the last 0.1–0.2 s of the calculation. Sensitivity studies were performed to determine the grid size dependency of results. No significant dependence was found for axial node sizes. The readers are referred to the studies of Pasamehmetoglu and Nelson (1991) and Pasamehmetoglu (1992) for more detailed information for the numerical scheme and accuracy.

The surface topography model used as an input to the boiling heat transfer program is discussed next.

III. SURFACE TOPOGRAPHY MODEL

To distribute the cavities over a boiling surface, we used a Monte Carlo scheme. First, we assumed that all the cavities were conical in shape. This is merely an assumption and is based on the abundance of literature dealing with conical cavities and the simplicity of this geometry. The discussion that follows would not be qualitatively the same with the choice of any other idealized geometry. Obviously, real geometries would have a considerably more complicated topography model, but there is not sufficient empirical data for the choice of such complicated geometries. Such complications would possibly overwhelm the subsequent results and would not add much to our parametric analysis. Having made the choice of conical cavities, two geometric parameters must be determined for the cavity radius and cone angle.

The cavity radii are obtained using a exponential probability density function, given by

$$\text{pdf}\,(R_c) = \frac{1}{R_{c,m}} \exp\left(-\frac{R_c}{R_{c,m}}\right), \tag{1}$$

where $R_{c,m}$ is the mean cavity radius and is varied parametrically between 1 and 10 μm in the current calculations. The exponential distribution was suggested by the experimental study of Yang and Kim (1988). Their measured mean and maximum cavity radii were 1.03 and 3.0 μm, respectively. We plotted the cumulative number densities obtained using Eq. (1) for a mean cavity radius of 1 μm in Fig. 3 along with data of Yang and Kim (1988) and our Monte Carlo simulation results. The Monte

Carlo simulation result presented in Fig. 3 considers two cases for a mean cavity radius of 1 μm. In each case, the total number of cavities on the heater surface was 100. As we will discuss later, the selection of seed number for the Monte Carlo simulation is an important statistical parameter for defining the cavity distribution curve. Cases considered in Fig. 3 use care for seed numbers that result in minimum and maximum wall superheats.

Figure 3 shows that the Monte Carlo simulation results are in reasonable agreement with the exponential cumulative distribution curve. For both seed numbers, the deviation from the exponential cumulative distribution curve is much less than the deviation of measured data from the exponential cumulative distribution curve. As we will mention later, this change could cause a relatively significant change in the wall superheat. It is difficult to claim that the exponential distribution is universal for all surface finishes. However, in view of the lack of further information, we believe the current approach is as suitable as any other for the parametric study of interest.

The second independent geometric parameter is either the cone depth or the cone angle. We chose to model the cone angle using a normal distribution also suggested by Yang and Kim (1988). Obviously, this is also a distorted distribution, since negative cone angles are not permissible. Normal distribution is a two parameter distribution where the mean and standard deviations must be defined. Note that the cavity cone angle does not directly enter into the boiling heat transfer calculations. We use Bankoff's (1958) criterion to determine whether a cavity could be a potential nucleation site. For a cavity to be potentially active, we must have

$$\theta < 2\beta \ ,$$

where θ is the contact angle and β is the half-cone angle determined statistically using the normal distribution. In the current calculations, the contact angle is treated as a constant defined explicitly. If the above criterion is not met, the cavity is assumed to be flooded and not allowed to activate during boiling.

As discussed before, because we can accommodate only one cavity per active cell, it is difficult to convert the above statistics to a line-averaged value of roughness (CLA or RMS), which is commonly used in reporting the roughness of boiling surfaces. These are length-weighted averages, and when only one cavity is present over a length of ~2.5 mm (as it is the case for the current study), the resulting roughness values are unrealistically small. However, the above statistics can be converted to a mean-peak-to-valley height (referred to as R_z in German standards (Batheau 1992, Bier et al. 1978). Within the context of our model, R_z simply refers to the arithmetic average of the conical cavity depths. It appears that some of the boiling heat transfer data may be correlated as a function of the parameter R_z. However, later we will show that R_z as a single parameter is not sufficient to model roughness effects on the nucleate boiling.

In some calculations, we used an approximate approach where more than one cavity is allowed in a computational cell. We used a normal distribution with a mean number of cavities N_m and a standard deviation of σ_N to determine the number of cavities in a given computational cell. (For the case where there is only one cavity in the cell, $N_m = 1$ and $\sigma_N = 0$.) We assumed that all these cavities are at or near the center of the computational cell, and the cavity with the largest radius is the most favorable. Obviously, the most favorable cavity is a function of the wall superheat (see, for instance, Han and Griffith 1965). In our numerical model, the most favorable cavity is an input to the thermal transport solution and is not interactive. With minor modifications to the computer program, this interaction could be implemented. However, considering the approximate nature of the

approach and the unrealistic assumption that all cavities are at or near the center (fixed control volume), the refinement of this approach would be mostly academic.

Another arbitrary assumption is the normal distribution for the number of cavities in a given cell. This arbitrary approach is further influenced by truncating the resulting number to the nearest integer. This point is illustrated in Fig. 4, which shows the cumulative number of potential cavities as a function of cavity radius for two cases. For each case, the mean cavity radius, 10 μm, was kept constant. When $N_m = 1$ and $\sigma_N = 0$, the total cumulative number of cavities was estimated as 100. For the other case that considered $N_m = 4$ and $\sigma_N = 2$, because of the above mentioned truncation, the total cumulative number of cavities was estimated as 91, indicating that the normal probability function found no cavity for some of the heater cells. It is worth noting that for the latter case, the cumulative number for the smaller cavity radius was decreased, indicating the existence of larger cavities. As will be mentioned later, the increase in the population of cavities with a larger radius will increase the heat transfer coefficient and correspondingly decrease the wall superheat. Perhaps a better approach would be to use a discrete Poisson distribution. Sultan and Judd (1978) observed that the active site distribution on a boiling surface follows a Poisson distribution. However, this observation is valid for active sites only (consequently, it is a function of the thermal transport). Furthermore, Sultan and Judd (1978) showed that the claim of Poisson distribution for the active sites is influenced by how we choose the size of subareas. Consequently, we believe the current approach (considering the limitation imposed by a fixed grid) is as good as any in terms of investigating the qualitative effects. However, this is an area where further improvements are possible in the numerical model.

IV. RESULTS AND DISCUSSIONS

Some of the results obtained from the numerical simulations are reported in this section. As mentioned before, in all the calculations reported in this paper, we simulated a 1-mm-thick copper heater. A 2.4-x-2.4-cm boiling area is modeled, which is divided into 10 x 10 computational cells (2.4 mm is the bubble departure diameter and is equal to the cell size). The power is supplied to the heater as a constant heat flux from the bottom boundary, and the boiling occurs on the top surface. Sensitivity of the boiling curve on the heater material, heater thickness, and the heating methods also are investigated during the course of this study. However, including the results of all those calculations within a single paper was impossible, and those subjects will be treated separately in subsequent papers.

In the first set of calculations, we allowed only one cavity per computational cell ($N_m = 1$ and $\sigma_N = 0$). The cavity radii are distributed exponentially where the mean cavity radius is varied between 1 and 10 μm. Also, the cone angle is assumed constant for all cavities ($\beta_m = 20°$ and $\sigma_\beta = 0.0°$). The contact angle is assumed as 60°; thus, all the cavities are potential cavities and can be activated if the thermal conditions are favorable. The calculations are repeated for three heat flux levels: 100, 150, and 200 kW/m^2. The resulting boiling curves are shown in Fig. 5. As shown, the boiling curve shifts to the left with increasing $R_{c,m}$. In addition, the boiling curves become steeper with increasing $R_{c,m}$. In general, within the range investigated, we can approximate all the curves by a curve-fit in the form

$$q = C_1 (\Delta T_w)^{a_1} \ ,$$

where C_1 decreases with increasing $R_{c,m}$ and a_1 increases with increasing $R_{c,m}$.

As indicated before, in these calculations, one cavity per computational cell is used. Thus, there are a total of 100 cavities on the surface. Because of such small

population size, we investigated the sensitivity of the results to our Monte Carlo model. We repeated the calculations seven different times using different seeds for the random number generator. All the calculations shown in Fig. 5 are obtained using the same seed number that resulted in maximum wall superheat within the sample of seven calculations. The wall superheat range did not show very significant sensitivity for higher values of N_m. The temperature variation owing to different seed numbers became as high as 2°C when smaller N_m was used.

For the case of $R_{c,m} = 1$ μm, we plotted the cumulative number of cavities as a function of R_c in Fig. 3, for the two seed numbers, 10 and 55. Those seed numbers resulted in the minimum and maximum wall superheats. The cumulative number densities are quite similar. The uncertainties involved fit the experimental data to a given statistical distribution (i.e., the exponential distribution in this case). However, deviation in excess of 2°C in the wall superheat for a given heat flux is observed with this small variation in the statistics. Note that, in the study of Yang and Kim (1988), a sample of 50 cavities was used in determining the statistics for the cavity size. Those 50 cavities were observed over a 15 mm x 25 mm area of the heater. Thus, the discrepancy between the postulated exponential distribution and the data was far greater than the difference between the two curves, as shown in Fig. 3. Incidentally, the experimental mean cavity radius for the data of Yang and Kim (1988) was a little greater than 1 μm. Thus, it can be stated that our model is a good representation of a mirror-finished surface for a mean cavity radius of 1 mm. The results suggest that one has to be careful in using the statistical data. It appears that even small variations in the statistical parameters (especially in cavity radii for smooth surfaces) may result in noticeable differences in the boiling curve. Large samples are required to obtain meaningful statistics in reference to the surface topography effects on the boiling curve.

We repeated the similar boiling curve calculations using $N_m = 2$ ($\sigma_N = 1$) and $N_m = 4$ ($\sigma_N = 2$). The resulting boiling curves are shown in Figs. 6 and 7. As shown, increasing N_m squeezes the boiling curves together. Because the possibility of a potential cavity with a larger radius increases with increasing N_m (see Fig. 4), the boiling curve for a given $R_{c,m}$ moves to the left. This shift is more pronounced at a lower value of mean cavity radius and becomes relatively insignificant at a higher value of mean cavity radius. This is because when N_m is increased for a larger mean cavity radius, the possibility of having a significant variation in larger cavity population decreases. Thus, for a higher value of $R_{c,m} = 10$ μm, increasing N_m has very little effect on the boiling curve because it is very likely that each cell containing a potential site will show less variation in cavity radius and will be relatively independent of N_m. Actually, because of one of our simplifying assumptions, for the case of $R_{c,m} = 10$ μm, increasing N sometimes results in an adverse effect where the wall superheat for a given heat flux increases with increasing N_m. This feature is discussed further in the next paragraph. We must note that, when we repeated the calculations for $N_m = 4$ using different seed numbers for the random number generator, the difference between minimum and maximum predicted superheats was less than 1°C.

Another way of plotting Figs. 5, 6, and 7 would be to plot the wall superheat as a function of $R_{c,m}$ for a constant heat flux. Such plots are shown in Figs. 8 and 9 for $q = 100$ kW/m^2 and $q = 200$ kW/m^2, respectively. These figures show that the wall superheat decreases with increasing $R_{c,m}$ approaching an asymptote. This behavior is very similar to the experimentally observed behavior reported by Corty and Foust (1955), where the wall superheat is plotted as a function of RMS roughness for a constant heat transfer coefficient ($q/\Delta T_w$). Unfortunately, it is difficult to quantitatively compare the two results because of the difficulties of converting the $R_{c,m}$ value to RMS roughness, as discussed previously. On the other hand, we

mentioned previously that $R_{c,m}$ can be converted to the mean-peak-to-valley height (R_z), which is a roughness measure commonly used in the German standards. These results indicate that, while the heat transfer coefficient increases with R_z, R_z alone is not sufficient to characterize the boiling curve. As shown in this figure, within the narrow range investigated, N_m also has a strong influence, confirming the observations of Chowdhury and Winterton (1985).

Figures 8 and 9 show some peculiar behavior for $R_{c,m}$ = 10 mm. As shown in both figures, the wall superheat for N_m = 2 is greater than the wall superheat for N_m = 1, for $R_{c,m}$ = 10 μm. As we mentioned before, when a normal probability function is used to distribute the number of cavities for each cell, because of the truncation of numbers, some cells could result in having no cavity. For these cases, the cumulative number density is less than 100, as illustrated in Fig. 4. Thus, the predicted wall superheat could deviate from the expected trend.

Figures 10 and 11 show the effect of the standard deviation in cone angle on the boiling curve. As shown, increasing the standard deviation increases the cone angle for some of the cavities. The cavities with large cone angles are flooded and consequently can not activate. Thus, the boiling curve shifts to the right with increasing σ_β. The same trend is observed for N_m = 1 and N_m = 4. However, increasing N_m increases the probability of a potential cavity with a relatively larger radius in each cell. Consequently, the boiling curves are less sensitive to σ_β for N_m = 4 (Fig. 11) than they are for N_m = 1 (Fig. 10). Similar behavior is observed for calculations repeated using different values of R_m. In these calculations, a contact angle of 60° is assumed between the copper surface and water.

Another parameter that results in the same type of shifts for the boiling curve is the contact angle. By changing the contact angle from 60° to 40°, the boiling curves shift to the right, as shown in Fig. 12. As shown, the sensitivity increases with decreasing number of cavities and with a decreasing mean cavity radius.

V. SUMMARY AND CONCLUSIONS

The effect of surface topology on the saturated pool nucleate boiling curve was studied parametrically using a numerical simulation model. The numerical simulation consisted of solving the three-dimensional transient heat conduction equation within the heater subjected to nucleate boiling over its upper surface. A finite-control volume approach with octagonal cells was considered to simulate a single bubble.

The surface topography model to distribute the cavities and cavity angles over the boiling surface used a Monte Carlo scheme. All cavities were assumed to be conical in shape. Each octagonal cell was considered to have a number of cavities obtained from a normal distribution with a known standard deviation. However, only one cavity with the largest cavity radii was assumed to be activated for each octagonal cell. The cavity radius is obtained using a exponential probability density function with a known mean value. The cavity cone angle for each cavity was determined using a normal distribution and required the mean cavity angle and its standard deviation to be specified. To determine the potential cavities for activation, Bankoff's (1958) cavity flooding criterion is used.

Parametric results showed that the saturated nucleate boiling curve shifted left and became steeper with an increase in the mean cavity radii when a constant cavity angle and total number of cavities are considered. Calculated boiling curves could be correlated with the classical approach $q = C(\Delta T)^a$. The coefficient C decreased with increasing mean cavity radii, and the exponent *a* increased with increasing mean cavity radii.

The boiling curve was found to be sensitive to the selection of the number of cavities for each octagonal cell. A small variation in the statistical parameters, especially cavity radii for smooth surfaces, resulted in noticeable differences in wall

superheat for a given heat flux. This result indicated that while the heat transfer coefficient increased with cavity radii, corresponding to cavity height (or roughness), the cavity radii or height alone is not sufficient to characterize the boiling curve, as previously suggested by Chowdhury and Winterton (1985). It also suggested that statistical experimental data should consider large samples to characterize the surface topology.

The boiling curve was shifted to the right when the cavity angle was obtained using a normal distribution. This effect became less important when the number of cavities for each cell was increasing owing to the fact that the probability of the potential cavity with a larger cavity radii in each cell was increased. When the contact angle of the fluid decreased for a given mean cavity radii, the boiling curve shifted to the right. This shift was more pronounced at smaller mean cavity radii and decreased with increasing mean cavity radii.

The paper illustrates that the simple numerical simulation model is capable of predicting most of the parametric trends of the nucleate boiling curve. Obviously, a finite control volume approach with a fixed grid has certain limitations in simulating the real surface topography. In addition, the data comparison is difficult because a single parameter roughness data CLA or RMS is difficult to convert to topography (the parameters of interest are those such as cavity shape, angle, radii, and number density needed).

REFERENCES

Bankoff, S. G., 1958, "Entrapment of Gas in the Spreading of a Liquid Over a Rough Surface," *A.I.Ch.E. J.* **4**, 24–26.

Barthau, G., 1992, "Active Nucleation Site Density and Pool Boiling Heat Transfer - An Experimental Study," *Int. J. Heat Mass Transfer* **35**, 271–278.

Bier, K., Gorenflo, D., Salem, M., and Tanes, Y., 1978, "Pool Boiling Heat Transfer and Size of Active Nucleation Centers for Horizontal Plates with Different Surface Roughnesses," *Proc. 6th Int. Heat Transfer Conf.*, (Toronto, Canada, August 7–11, 1978), Vol. 1, pp. 151–156.

Chowdhury, S. K. R. and Winterton, R. H. S., 1985, "Surface Effects in Pool Boiling," *Int. J. Heat Mass Transfer* **28**, 1881–1889.

Cole, R. and Rohsenow, W. M., 1969, "Correlation of Bubble Departure Diameters for Boiling of Saturated Liquids," *Chem. Eng. Prog. Symp Series*, No. 92, Vol. 65, pp. 211–213.

Corty, C. and Foust, A. S., 1955, "Surface Variables in Nucleate Boiling," *Chem Engng Prog. Symp. Ser.*, No. 17, Vol. 51, pp. 1–10.

Dhir, V.K., 1990, "Nucleate and Transition Boiling Heat Transfer Under Pool and External Flow Conditions," 9th International Heat Transfer Conference Proceedings, KN-9, pp. 129-154, Israel, 1991, International Journal of Heat and Fluid Flow, Vol. 12, No. 4, pp. 290–314, December.

Han, C-Y and Griffith, P., 1965, "Mechanisms of Heat Transfer in Nucleate Pool Boiling, Part II: The Heat Flux—Temperature Relationship," *Int. J. Heat Mass Transfer* **8**, 905–914.

Jacob, M., 1949, *Heat Transfer* (John Wiley and Sons, New York).

Pasamehmetoglu, K. O., 1992, "Numerical Modeling of a Nucleate Boiling Surface," submitted to *Numerical Heat Transfer, Part A: Applications.*

Pasamehmetoglu, K. O. and Nelson, R. A., 1991a, "A Finite Control Volume Computer Program for Heater Analysis of Nucleation Dynamics (HANDY)," Los Alamos National Laboratory Report LA-UR-91-977 (January 1991).

Pasamehmetoglu, K. O. and Nelson, R. A., 1991b, "Cavity-to-Cavity Interaction in Nucleate Boiling: Effect of Heat Conduction within the Heater," *AIChE Symposium Series*, No. 283, Vol. 87, pp. 342–351.

Sultan, M. and Judd, R. L., 1978, "Spatial Distribution of Active Sites and Bubble Flux Density," *ASME J. Heat Transfer* **100**, 56–62.

Thomas, T. R., 1981, *Rough Surfaces*, (Longman Inc., New York).

Wang C. H. and V. K. Dhir, 1991, "Effect of Surface Wettability on Active Nucleation Site Density during Pool Boiling of Water on a Vertical Surface," Phase Change Heat Transfer, ASME, HTD-Vol. 159, pp. 89–96.

Yang, S. R. and Kim, R. H., 1988, "A Mathematical Model of the Pool Boiling Nucleation Site Density in Terms of Surface Characteristics," *Int. J. Heat Mass Transfer* **31**, 1127–1135.

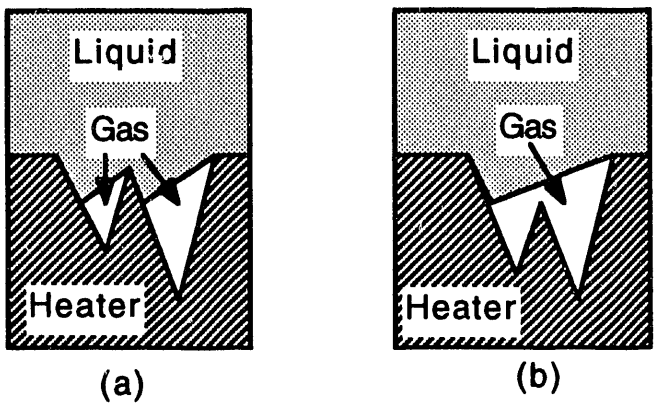

Fig. 1. The role of adjacent cavities in bubble nucleation.

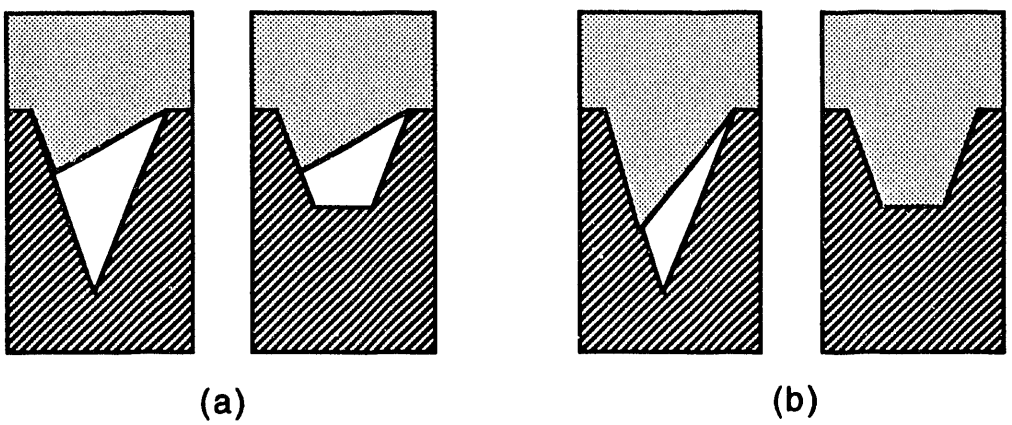

Fig. 2. Influence of the cavity shape on the boiling curve.

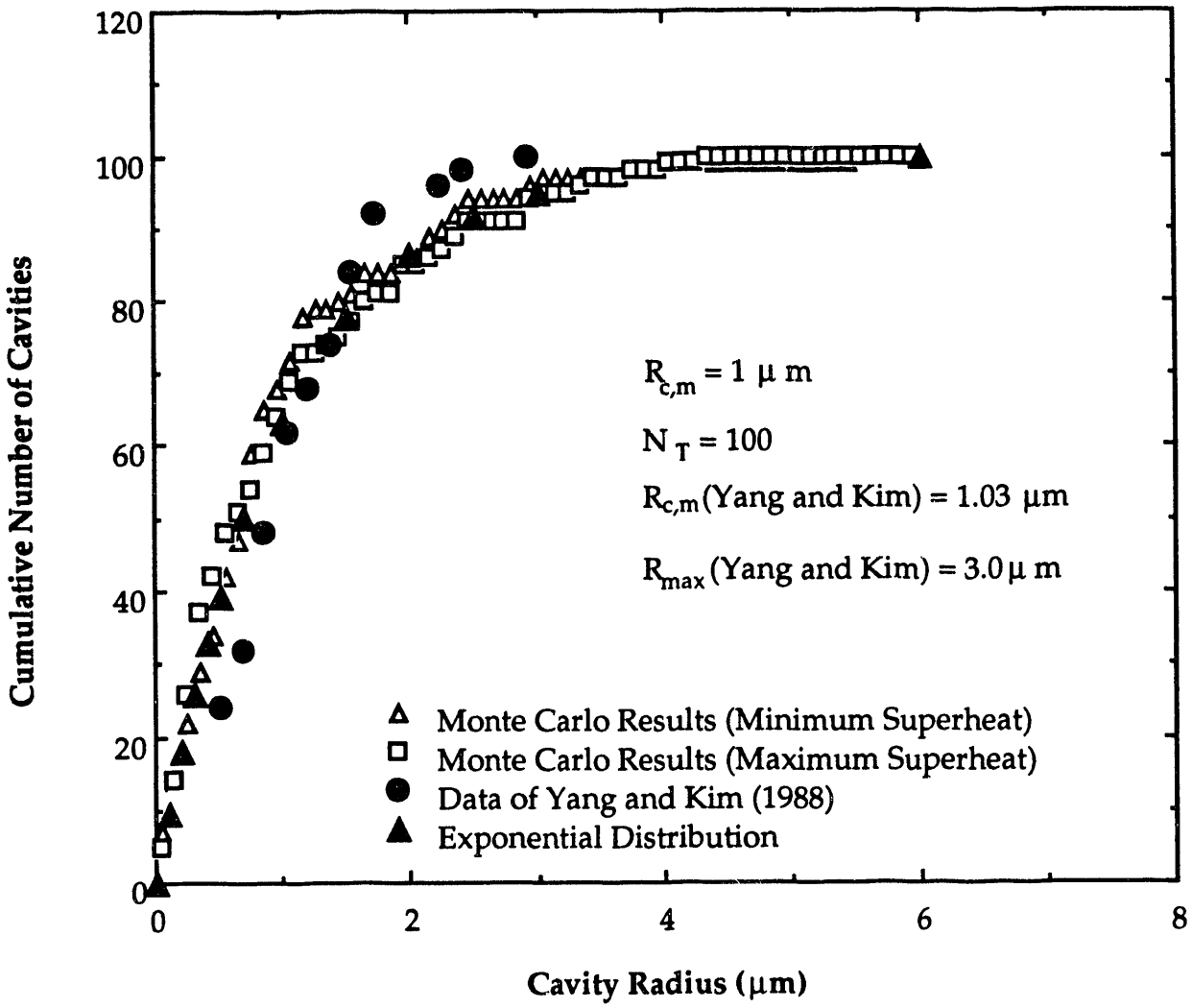

Fig. 3. Calculated cumulative number of cavities obtained from the Monte Carlo simulation and the exponential probability function, along with measured data of Yang and Kim (1988).

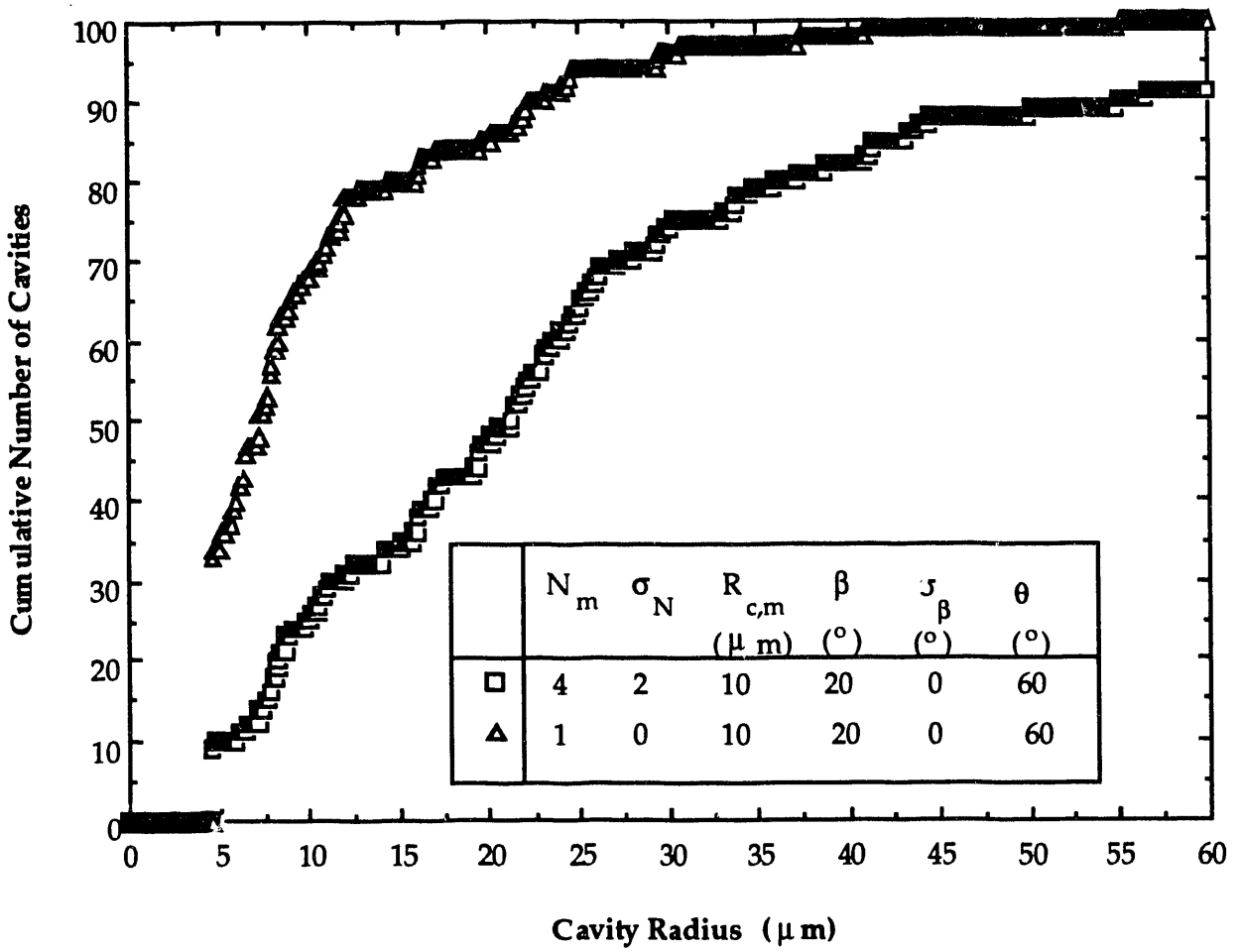

Fig. 4. Cumulative number of cavities for two different values of the number of cavities per orthogonal cell (N_m) for a mean cavity radius ($R_{c,m}$) of 10 μ.

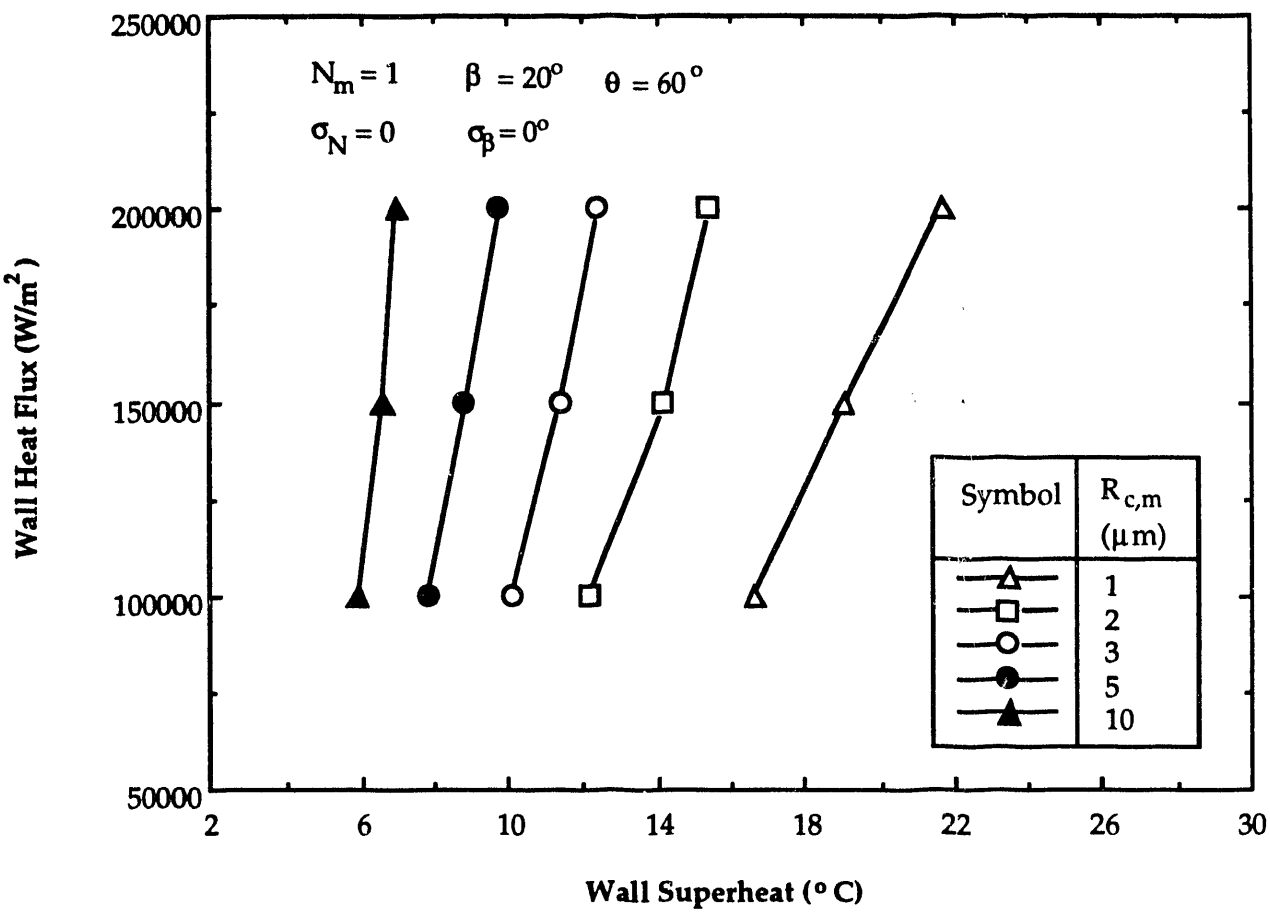

Fig. 5. Calculated boiling curves for a mean cavity radii range of 1–10 μ using a constant β, N_m, and θ.

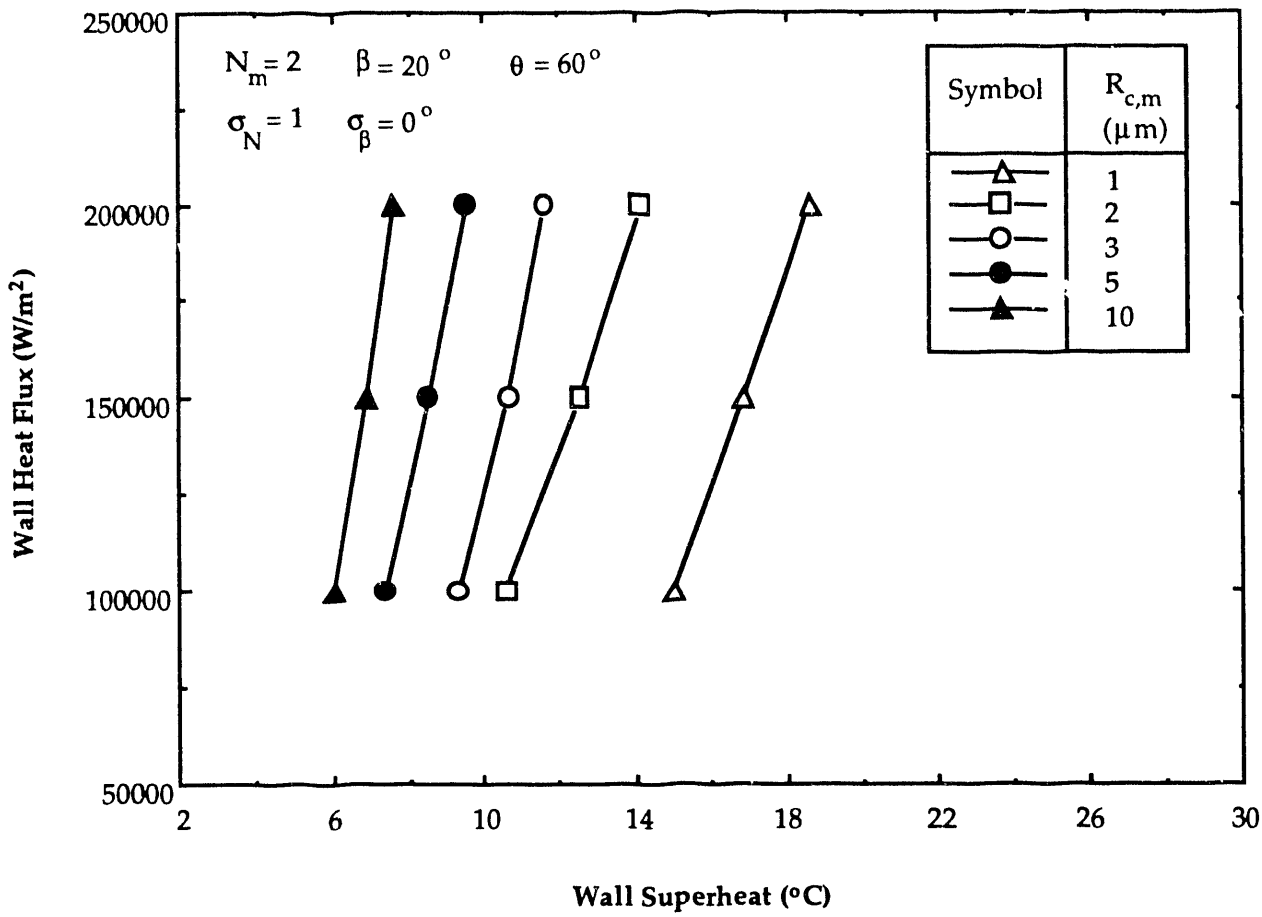

Fig. 6. The influence of the number of cavities per octagonal cell on the boiling curves, $N_m = 2$, when β and θ are constant.

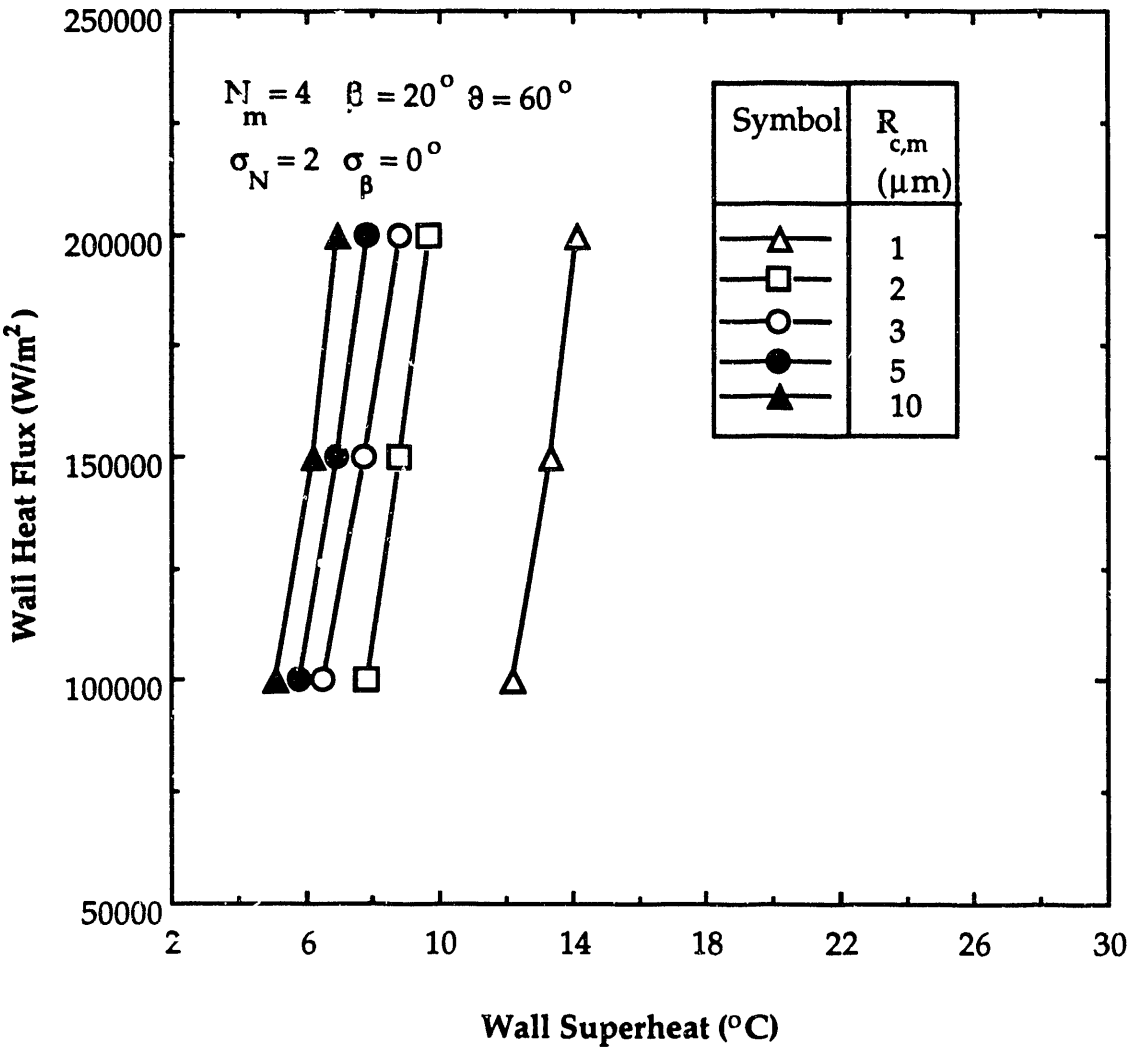

Fig. 7. The influence of the number of cavities per octagonal cell on the boiling curves, $N_m = 4$, when β and θ are constant.

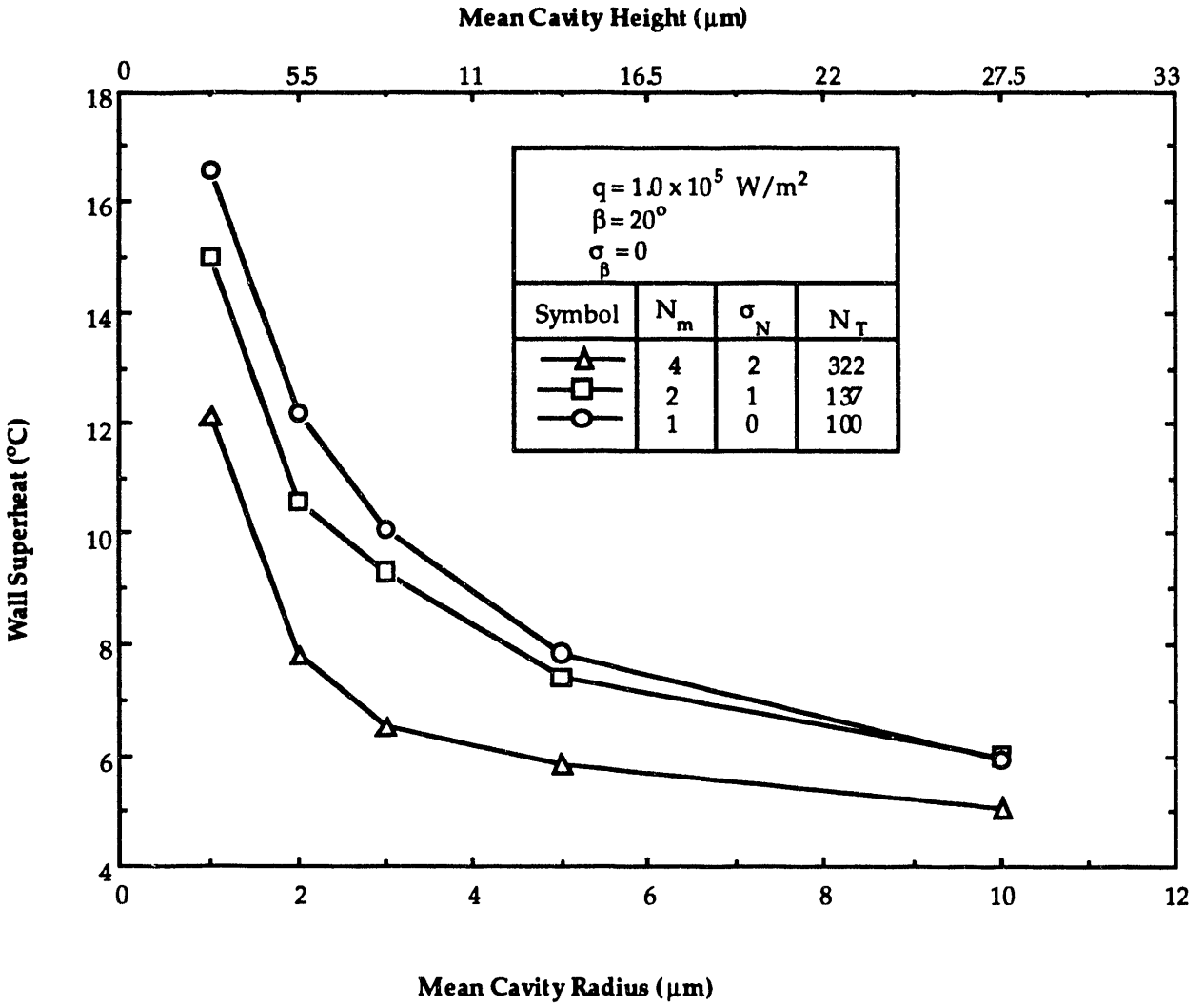

Fig. 8. Calculated wall superheats as a function of mean cavity radius at a heat flux level of 1.0×10^5 W/m^2 for three different N_m.

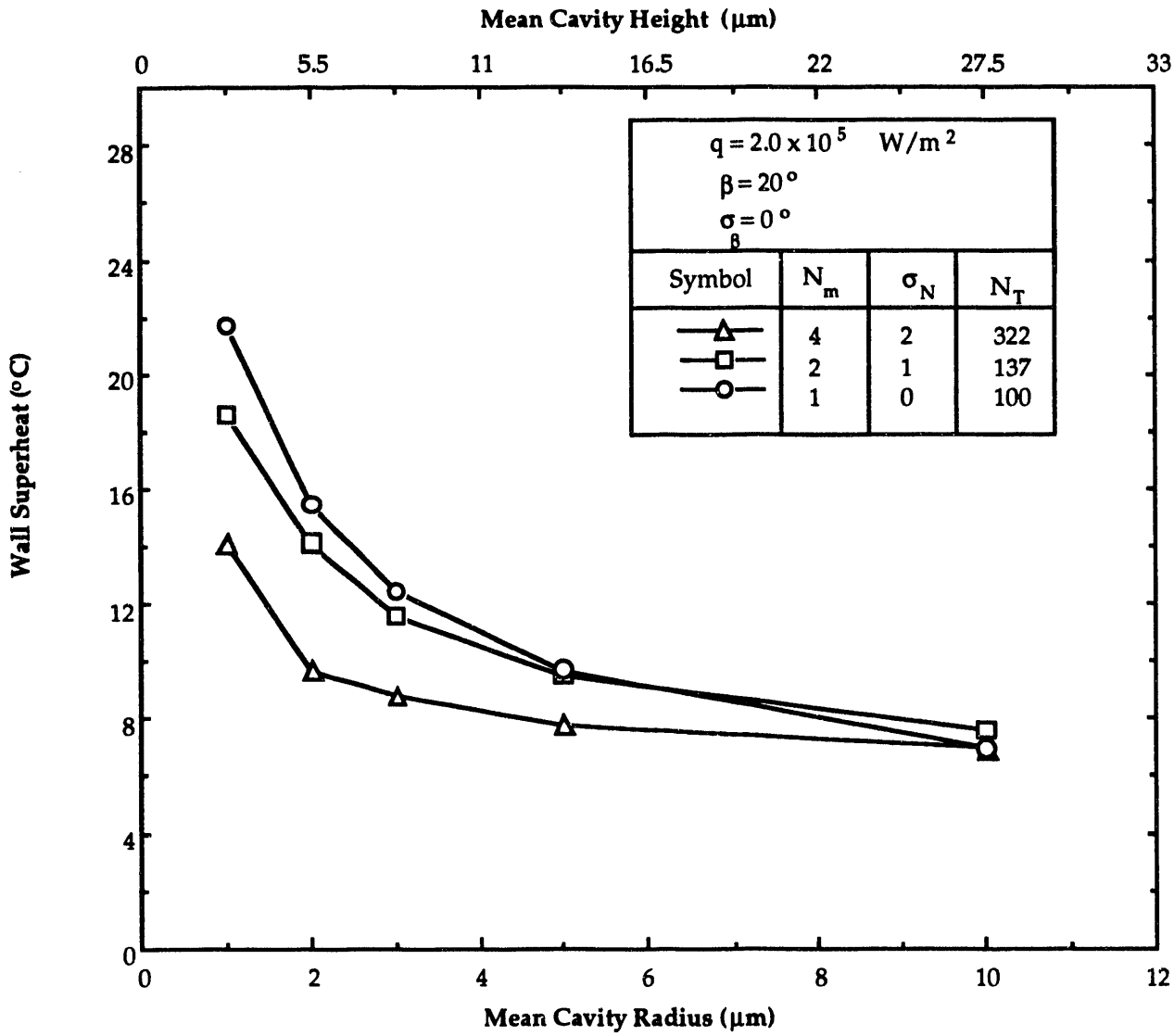

Fig. 9. Calculated wall superheats as a function of mean cavity radius at a heat flux level of 2.0 x 10^5 W/m^2 for three different N_m.

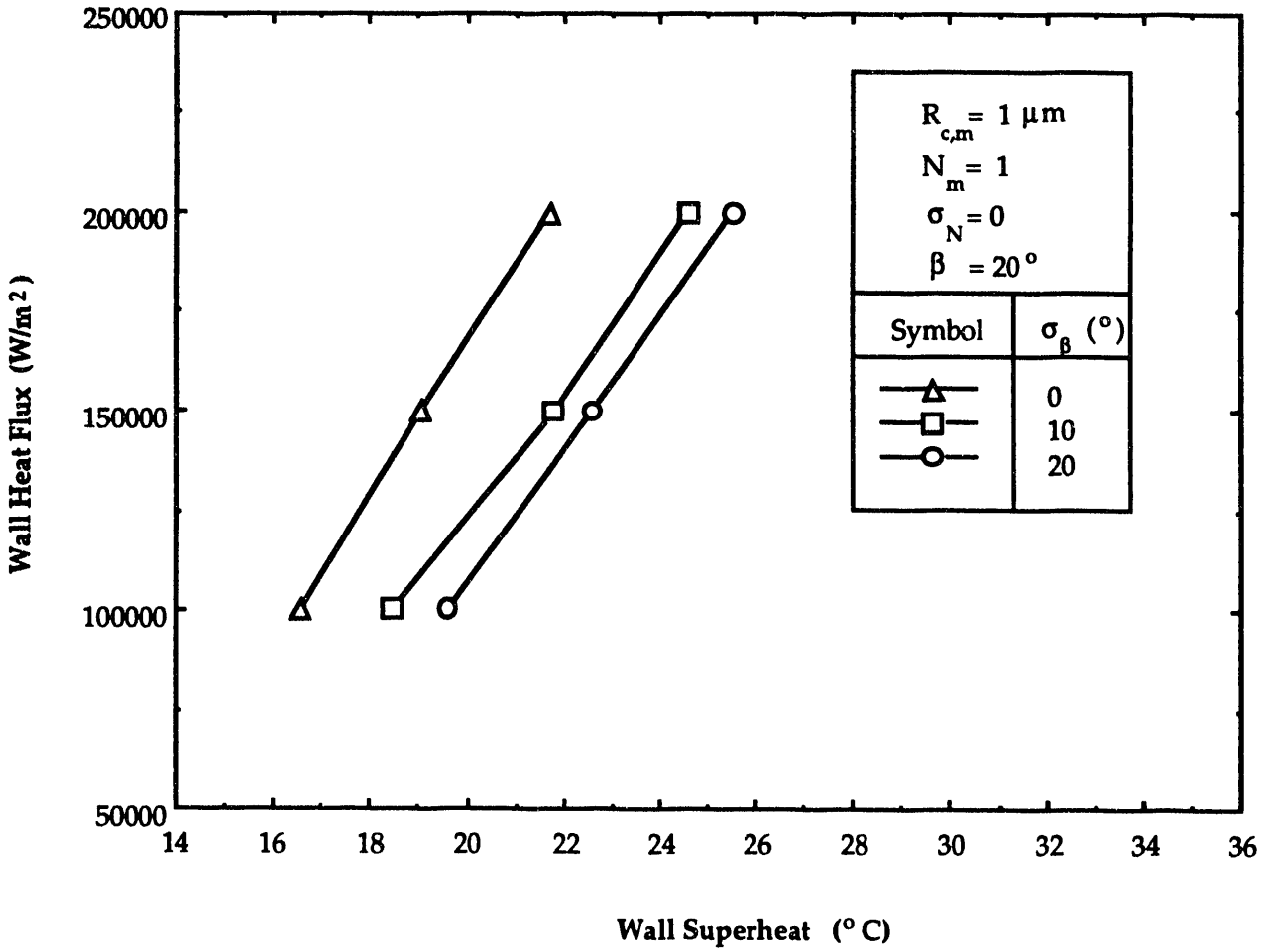

Fig. 10. Calculated boiling curves when the cavity cone angle is calculated from a normal probability function using three different standard variations for $N_m = 1$ and $R_{c,m} = 1\ \mu$.

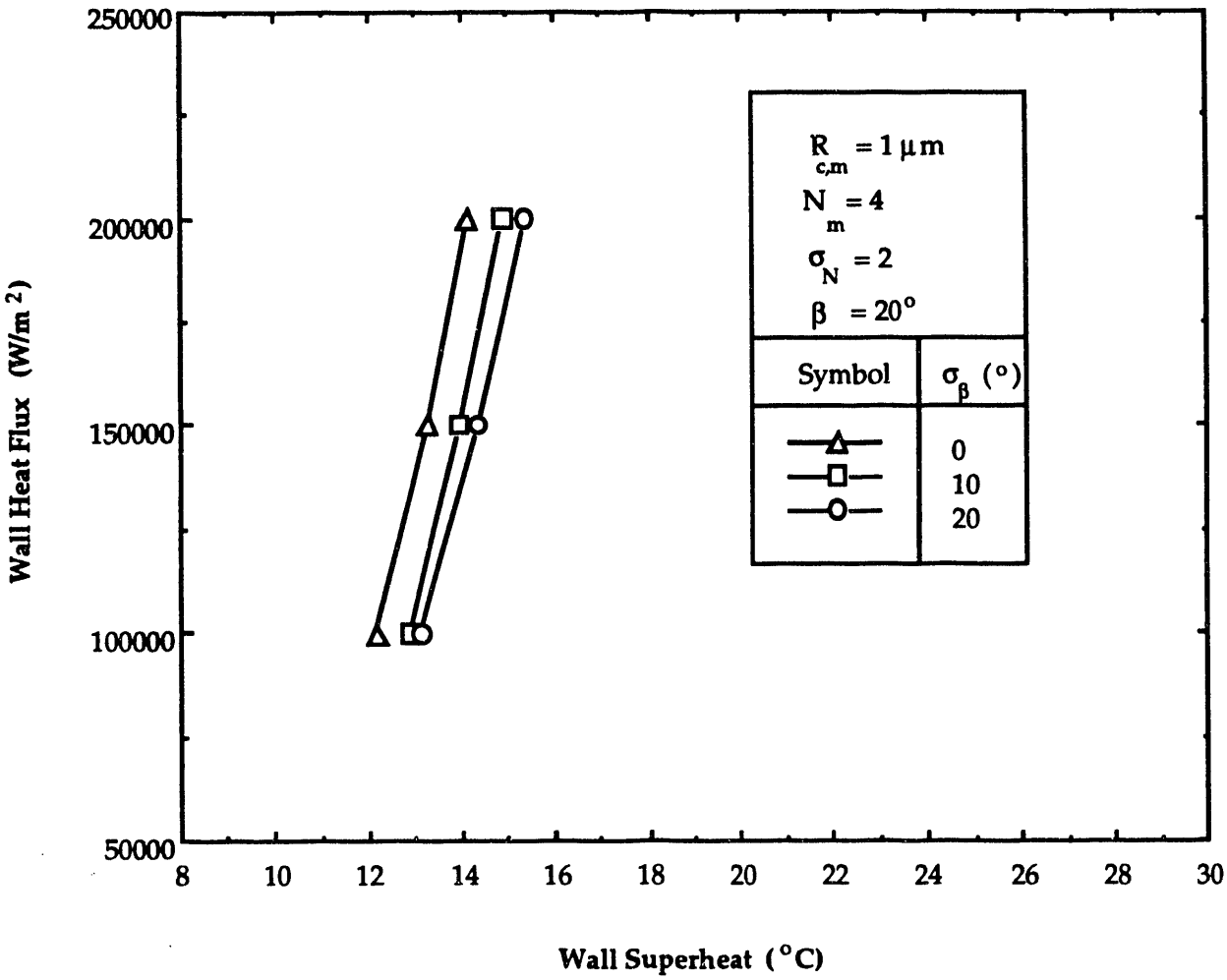

Fig. 11. Calculated boiling curves when the cavity cone angle is calculated from a normal probability function using three different standard variations for $N_m = 4$ and $R_{c,m} = 1\ \mu$.

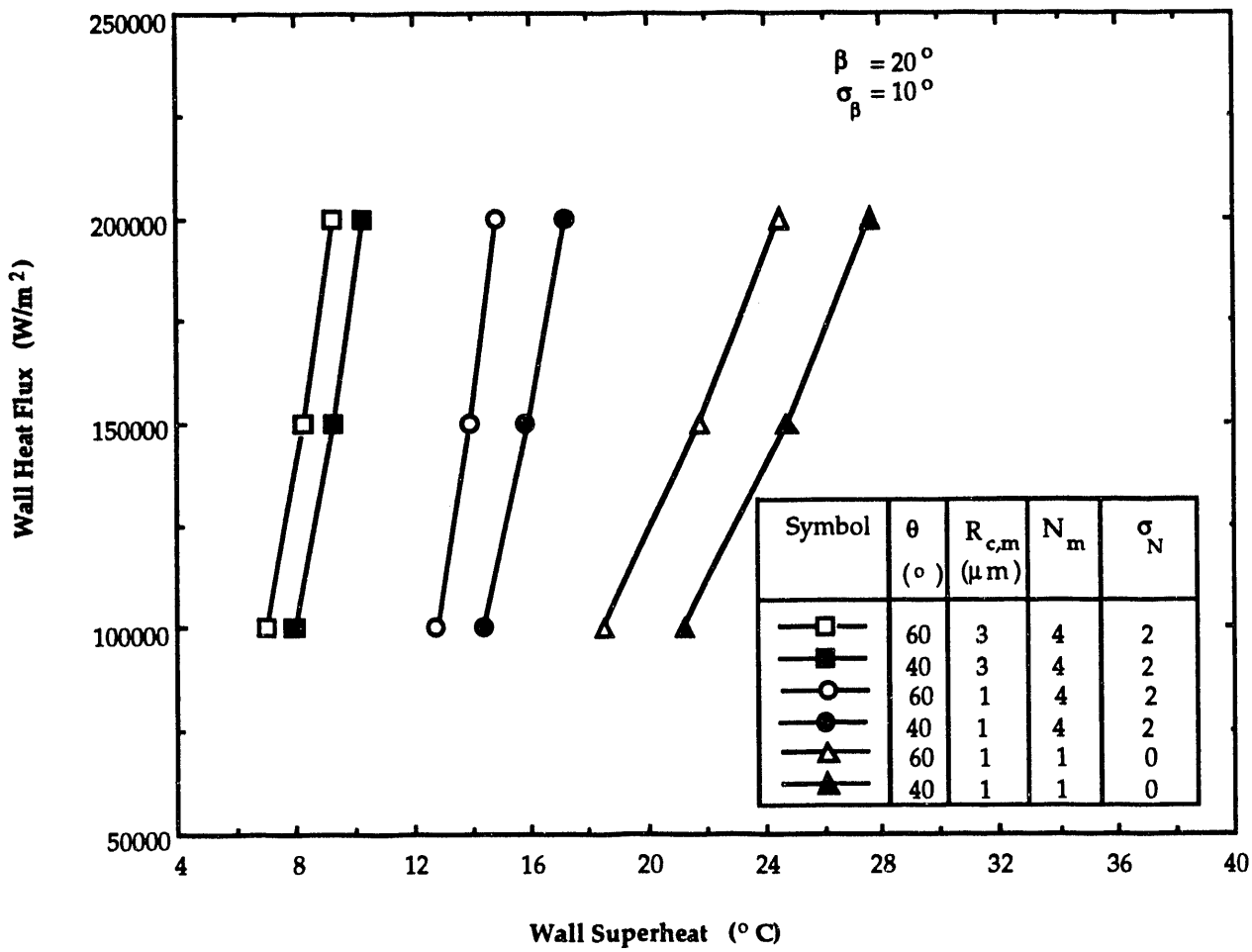

Fig. 12. The effect of the contact angle on the nucleate boiling curve.

END

DATE
FILMED
10/14/93